BOLTON, M. D. & PANG, P. L. R. (1982). *Géotechnique* **32**, No. 4, 349–367

Collapse limit states of reinforced earth retaining walls

M. D. BOLTON* and P. L. R. PANG†

The use of systems of earth reinforcement or anchorage is gaining in popularity. It therefore becomes important to assess whether or not the methods of design which have been adopted for such constructions represent valid predictions of realistic limit states. Confidence can only be gained with regard to the effectiveness of limit state criteria if a wide variety of representative limit states has been observed. To clarify the nature of appropriate collapse criteria, over 80 centrifugal model tests of simple reinforced earth retaining walls have been carried out. Collapses due to insufficient friction have been shown to be repeatable and are therefore subject to fairly simple limit state calculations. However, a series of well-instrumented models showed that whereas the first occurrence of ultimate tensile strength in a strand of reinforcement was always reliable and was subject to a conservative limit state calculation after the fashion of Rankine, the ultimate collapse condition was less reliable owing to progressive collapse if the reinforcing elements were brittle or had local weak spots. The long-term limit state of a full-scale reinforced earth structure is even more likely to be associated with the first fracture of some weak bolted joint or localized zone of corrosion. Calculations of such limit states should therefore not include Coulomb wedges or other surfaces of rupture along which the reinforcements are presumed simultaneously to offer their ultimate strength.

L'emploi de systèmes de renforcement ou d'ancrage du sol devient de plus en plus répandu. Il est donc important d'estimer si les méthodes adoptées pour de telles entreprises représentent des prédictions valables d'états-limite réalistes. L'assurance en ce qui concerne l'efficacité des critères d'état-limite ne peut être obtenue qu'après l'étude d'une grande variété d'états-limite typiques. Plus de 80 essais sur modèles centrifuges ont été réalisés sur des murs de soutènement simples renforcés, afin de définir des critères de rupture appropriés. On a démontré que les ruptures dues à une insuffisance de frottement peuvent être reproduites de sorte qu'elles fonds l'objet de calculs d'état-limite assez simples. Cependant, comme des séries de modèles bien instrumentés l'indiquent, bien que le premier cas de résistance à la traction définitive ait été toujours fiable et susceptible de former l'objet d'un calcul d'état-limite prudent suivant la méthode Rankine, l'état de rupture définitif était moins fiable, en raison de la rupture progressive si les éléments de renfort étaient cassants ou avaient des points de faiblesse localisés. L'état-limite à long terme d'une structure complète de sol renforcé sera encore plus probablement associé avec la première rupture de quelque joint faible fixé par boulon ou avec une zone localisée de corrosion. Les calculs d'état-limite de ce genre ne devraient donc pas comprendre des coins de Coulomb ou autres surfaces de rupture où l'on présume que les renforcements atteignent leur résistance définitive simultanément.

Discussion on this Paper closes on 1 March 1983. For further details see inside back cover.

* University Engineering Department, Cambridge.
† Allott and Lomax.

INTRODUCTION

Henri Vidal has achieved the distinction of conceiving, elaborating and popularizing a new technology in earth retention in only two decades. This development may be traced through Vidal (1966, 1969), Schlosser & Vidal (1969), Schlosser & Long (1974), Juran & Schlosser (1978) and Schlosser & Segrestin (1979). It is a tribute to these workers that the *Terre Armée* (Reinforced Earth) method of creating a rectangular retaining wall (Fig. 1) has become so familiar.

The symposium on earth reinforcement held in Pittsburgh in 1978 and the international conference on soil reinforcement in Paris in 1979 testified to the rate of exploitation of this method and the investigation of analogous systems. Patent holders and research workers have launched a diversity of design calculations for reinforced earth constructions. This Paper identifies those calculations which may form a part of a consistent limit state method.

Design requirements

The Institution of Structural Engineers' (1955) report on structural safety specified that the

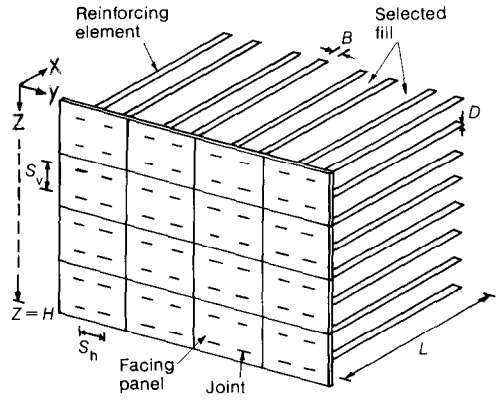

Fig. 1. Reinforced Earth retaining wall

following conditions were to be satisfied 'within a reasonable degree of probability' in the design of a structure

(*a*) the structure shall retain throughout its life the characteristics essential for fulfilling its purpose, without abnormal maintenance cost.
(*b*) the structure shall retain throughout its life an appearance not disquieting to the user and general public, and shall neither have nor develop characteristics leading to concern as to its structural safety
(*c*) the structure shall be so designed that adequate warning of danger is given by visible signs and that none of these signs shall be evident under design working loads.

It is now usual to define limit states of safety and serviceability and to perform calculations to demonstrate that the risk of any collapse, or of a given limiting degree of deformation, is acceptably small when forseeable variations in loads, materials and workmanship are taken into account. The requirement (*c*) would be satisfied only if certain pre-designated signs could be relied on to give a sufficient warning of danger, even when the cause was unforeseen. Building codes have generally taken this into account by requiring that the components and their joints behave in a continuous ductile fashion wherever possible, so that excessive unforeseen forces or unforeseen material degradation may be expected to cause excessive but controlled deformations which would alert the occupants and allow them to be evacuated. Components which would behave in a brittle manner, such as over-reinforced concrete beams, are usually proscribed. Joints which may snap or slide open, such as those at Ronan Point which allowed the progressive collapse of part of a residential multi-storey building due to an unexpected gas explosion in one room, are also banned.

Serviceability limit states

Reinforced earth is recognized to be a relatively flexible form of construction. This has led to reduced concern over possible damage due to differential settlements when assessing the likely performance of reinforced earth retaining walls in comparison with conventional cantilever retaining walls. A less desirable consequence is that greater deflexions may be expected in such a wall as it is built. It may be necessary to set out the face of the wall at a substantial inward rotation so as to account for the outward rotation which may occur during construction, and which could be of the order of 1/30 to 1/50 (Finlay and Sutherland, 1977). Construction gangs are quick to acquire the skill to execute such works within the required dimensional tolerances. This experience has led to the tacit acceptance that the designer of a reinforced earth retaining wall must have two main concerns: to avoid collapse limit states by good design and to avoid short-term serviceability limit states by insisting on skilful and observant site personnel. This Paper includes some data on deformations, but most new data will be concerned with the collapse of model reinforced earth walls.

Collapse limit states

Collapse limit states for reinforced earth retaining walls may be divided into five categories

(*a*) inclusion in a landslide: the stresses both within and on the boundary of the reinforced zone are not limiting, but the construction may trigger off collapse due to alterations of stress or pore-water pressure within the surrounding natural materials
(*b*) monolithic collapse: the stresses within the reinforced zone are not limiting, but stresses around its boundaries all approach limiting values so that the reinforced zone may grossly translate, subside or rotate as a monolith
(*c*) collapse by internal slippage: the stresses within the reinforced zone are limiting, such that gross distortions of the soil may occur, thereby triggering off a collapse
(*d*) collapse by tensile rupture of the reinforcement: the stresses within the reinforced zone are limiting, such that some reinforcement or its joint with a facing panel breaks in tension and thereby triggers off collapse
(*e*) collapse by rupture of the facing panels: the stresses on the front boundary of the reinforced zone are limiting, such that a facing panel disintegrates and triggers off a collapse.

It is also necessary to consider any interactions between these idealized modes of collapse. The first mode would usually be investigated with collapse mechanisms involving sliding surfaces and the method of slices would generally be used to find which mechanism possesses the smallest factor of safety. The second mode also draws on techniques previously well established for masonry retaining walls (Smith & Bransby, 1976). The remaining modes of collapse are exclusive to reinforced earth retaining walls.

The first clear statement of design methods based on the analysis of stresses or forces within a mass of reinforced earth was made by Schlosser & Vidal (1969). They proposed two methods; Fig. 2(a) shows their calculations based on Coulomb's trial wedges and Fig. 2(b) was derived from Rankine's treatment of lateral earth pressures. The authors noted that if the arithmetical trivia caused

by the discrete nature of the spacing of reinforcements are ignored, the two methods lead to the same conclusion regarding the total force on a vertical stack of reinforcements when the soil collapses, i.e.

$$\Sigma T = \tfrac{1}{2} K_a \gamma H^2 S_h$$

They also noted that, whereas Rankine's method showed that these ultimate tensions should be triangularly distributed, Coulomb's method apparently released its user from this constraint. They did not make it clear that, in the absence of shear forces on the boundary AB in Fig. 2(a), the application of Coulomb's method with the apex A of triangle ABC at successively shallower positions relating to each reinforcing layer, would independently have generated a reinforcing force proportional to depth. The foregoing calculation of reinforcement tensions; based on the complete mobilization of the strength of the intervening soil, was considered to be independent of the calculation of an individual reinforcement's ultimate tensile capacity considering possible tensile rupture or slippage.

Wedge analysis

The conventional method of predicting the collapse of steel frames or soil slopes is to postulate a collapse mechanism and to consider that all elements which are thereby disrupted have approached their ultimate strength. These 'upper bounds' plastic design methods are inherently optimistic—in two senses. First, the designer will be forced by practical considerations to curtail his search for possible mechanisms and to assume that his efforts must have led him to a close approach to the least favourable collapse mode. Second, the assumption that every component will simultaneously offer its full strength before collapse presumes a ductility and continuity of construction that may be difficult to achieve in practice. Banerjee (1975) outlined a conventional

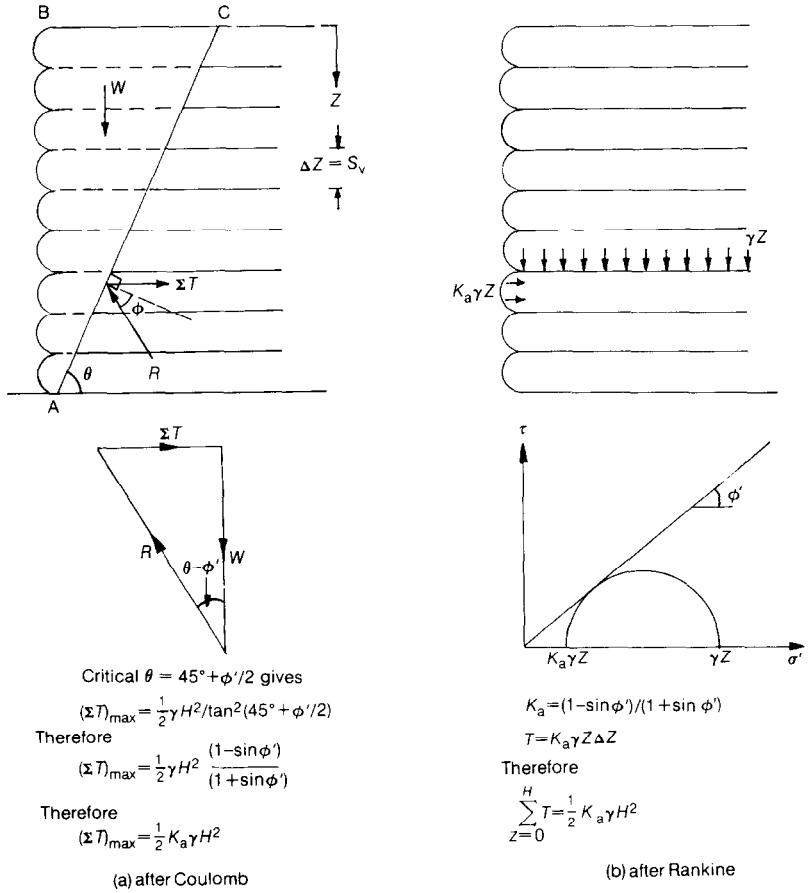

Fig. 2. Reinforcement forces per unit length (Schlosser & Vidal, 1969, figs 26 and 27)

upper-bound method in which, referring to Fig. 2(a), the sum of the strengths of all reinforcing members projecting beyond the trial wedge ABC was used in conjunction with the soil strength mobilized on the sliding surface AC in order to generate a safety factor which could be minimized with respect to the wedge angle θ. However, Schlosser & Vidal (1969) specifically avoided inferring the ultimate tensile capacity simultaneously in each of the reinforcing layers.

Stress analysis

The explanation for the avoidance of true upper-bound plasticity calculations by Schlosser & Vidal (1969) stems from their observation that 'failure of strips under the traction forces . . . does not happen by simultaneous failure of all the strips along a failure surface. The phenomenon is progressive, but very sudden: the most strained strip breaks, then after a redistribution of stresses, the next strip, etc.' This observation is emphasized by Schlosser & Long (1974): 'The method employed must be a local method making it possible to calculate the tensile stress in each layer of reinforcements independently of the stresses exerted in the other layers.' They developed a method based on the stress analysis of Fig. 2(b), modified to incorporate an increase in the stresses near the base of the facing due to the overturning moment on the reinforced zone created by its backfill.

Bolton, Choudhury & Pang (1978) pointed out that many features of this method were of the lower-bound plastic collapse type (Fig. 3). No collapse mechanism is employed, but the greatest

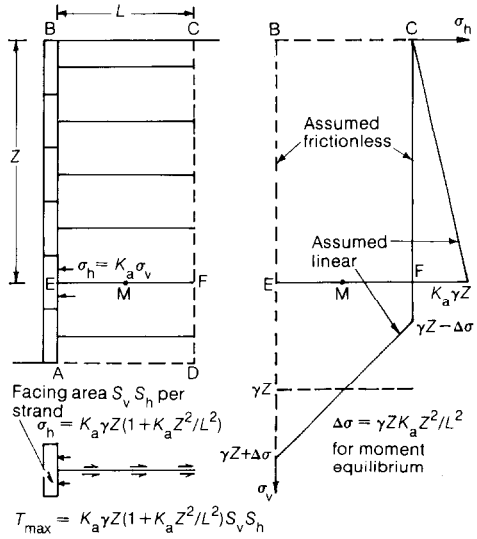

Fig. 3. Simple stress analysis: the anchor analogy

effort is made to determine a comprehensive field of stresses in equilibrium which nowhere defy the conditions of strength of the materials. The vertical faces BA and CD of the reinforced zone ABCD in Fig. 3 are taken to be perfectly frictionless; this must then create an analysis which is pessimistic relative to typical practical conditions, but which is made easier by the imposed condition that BA and CD shall be principal planes of stress. Unfortunately the complete stress analysis of a reinforced earth zone is beyond current capability, and so the specification of a trapezoidal base pressure distribution at any level such as EF which is at a depth Z is simply an attempt to ensure moment equilibrium about its midpoint M when the lateral pressures along CF are considered. Although the global equilibrium of BEFC is thereby achieved, there is no assurance that the material within can sustain, for example, the parabolic distributions of shear stress on EF dictated by this application of beam theory. Accepting this defect, the enforced conditions of vertical principal stress along BA and CD lead first to an enhanced vertical stress behind the element of facing with centroid at depth Z

$$\sigma_v = \gamma Z(1 + K_a Z^2/L^2) \tag{1}$$

and thereby to a horizontal stress on the facing

$$\sigma_h = K_a \gamma Z(1 + K_a Z^2/L^2) \tag{2}$$

where the active earth pressure coefficient is

$$K_a = \frac{1-\sin\phi'}{1+\sin\phi'} \tag{3}$$

and where a single value for ϕ' has been presumed for simplicity to apply to all the fill in and around the reinforced zone. The force developed on the element of facing of area $S_v S_h$ attributed to a single strand of reinforcement is therefore

$$T = S_v S_h K_a \gamma Z(1 + K_a Z^2/L^2) \tag{4}$$

If the structural connections between elements of facing are pessimistically assumed to transmit no forces, the force T must be transmitted directly to its tributary strand of reinforcement. Fig. 3 then indicates that inward acting shear stresses may be expected to cause the required reduction in tension from $T = T_{max}$ at the joint to zero at the free end of the strand. It follows that the safety factor against tensile failure of the reinforcement is predicted to be

$$F_T = \frac{P}{K_a \gamma Z S_v S_h (1 + K_a Z^2/L^2)} \tag{5}$$

where P is the lowest tensile strength in the region of the joint.

It is then necessary to introduce a second

assumption which may or may not be safe. If, at failure by slippage, the average shear stress developed on both surfaces of a flat horizontal strip can be as great as

$$\tau = \mu\gamma Z \tag{6}$$

where γZ is the average vertical stress over its length and μ is the coefficient of friction between soil and reinforcement determined by causing relative sliding in a shear box, then the total available frictional restraint of a strand of reinforcement is

$$Q = (2BL)\mu\gamma Z \tag{7}$$

and the safety factor against slipping is derived from the quotient of equations (7) and (4)

$$F_F = \frac{2BL\mu}{S_v S_h K_a(1 + K_a Z^2/L^2)} \tag{8}$$

Although the analysis leading to equations (5) and (8) is not wholly pessimistic, as a limit-state designer might wish, it certainly satisfies the requirement that each individual strand of reinforcement is assumed to be independent of the others, so that a limit state condition can be presumed when an anchor first satisfies either $F_T = 1$ or $F_F = 1$, even though the others may possess $F_T > 1$ and $F_F > 1$.

MODELLING COLLAPSE LIMIT STATES

Field tests

The only convincing way of demonstrating the safety of limit state criteria such as equations (5) and (8) is to generate a diversity of collapses and determine whether or not F_F or F_T were less than unity in all appropriate cases. Accuracy, and thence economy, would also be shown if on back-analysis F_F or F_T were not much less than unity. Full-scale instrumented collapses are expensive to create and difficult to control; only the single instrumented test is reported by Al-Hussaini & Perry (1978). Equations (5) and (8), converted for their 3·66 m high wall which effectively retained no soil but which was loaded by a uniform surcharge up to roughly 90 kN/m^2 at collapse, gave the values $F_T = 1{\cdot}32$, $F_F = 1{\cdot}66$. The sudden total collapse was preceded by a wall rotation which increased rapidly in the last 25% load increment up to about 1/30, and was evidently triggered off by a pattern of ruptures in the ties close to their joints, and of the joints themselves. The joints were assumed for the calculations to be as strong as the strips which they served, although they consisted only of two unspecified 6·4 mm dia. bolts acting in double shear through the 102 mm × 0·64 mm strip. The strength of the construction was evidently overestimated by about 30%.

Low-stress model tests

The validation of collapse limit state criteria has effectively been carried out solely by laboratory model tests. Schlosser & Vidal (1969) report a series of small (about 200 mm high) model walls supporting a quasi-soil of parallel steel needles by the insertion of aluminium tapes 0·009 mm thick. Lee, Adams & Vagneron (1973) studied more realistic models 200–500 mm high constructed in sand with ties cut from 0·013 mm aluminium foil. Layers of sand and strips were added in sequence until the model failed. Some instrumentation with strain gauges was attempted, although it was discovered that the backing strip and lead wires affected the stiffness of the parent tie, so that most gauges were located immediately behind the facing where their influence was minimized. Although these tests were sufficient to demonstrate the broad applicability of various limit state criteria, the quantity and quality of data were insufficient to discriminate between them. Particular problems were evident with data of tensile failure which suffered from scatter, and from an unexplained inability to differentiate between dense and loose sand. Tie breakages at the facing joint were possibly indicative of a local weakness that had not been measured.

Bacot & Lareal (1979) report earlier tests which were similar to those of Lee *et al.* (1973). No apparent attempt was made to measure reinforcement tensions, but collapse data were fitted accurately with a criterion derived from an adapted mechanism based on wedges. However, the fit was achieved by using $\phi' = 37°$ taken from triaxial tests on the uniform sand at a unit weight of 15 kN/m^3 and a confining pressure of about 100 kN/m^2. At the very low stresses implied by these 200–500 mm high walls, it might have been expected that even such a sand would have displayed considerable dilatancy and a plane strain value of ϕ' in excess of 40°. If the value $\phi' = 37°$ is accepted, however, the relatively pessimistic criterion of equation (5) would have underpredicted the tensile strength of Bacot & Lareal's models at collapse by a factor of up to 1·5. Juran & Schlosser (1978) refer to a series of models 100–400 mm high studied by Binquet & Carlier (1973). Although there was a difficulty caused by the need to discount the self-supporting tendency of the rigid facing elements which had been used, it seemed that the simple approach of Fig. 3 still underestimated the tensile strength of the models by a factor of roughly 1·8.

There have been two sorts of reaction to the apparent underprediction of some tension failures by stress analysis. Vidal (1978) wrote, 'On the other hand, we have been very disappointed by the results on models . . . which do not correspond to

the results of the real structure'. This does not make clear that he was drawing a comparison between collapse tests on models and field instrumentation of safe structures. It is not clear how measurements on a safe structure relate to collapse limit states. If model tests of collapse are flawed, moreover, how can the factor of safety of existing structures be assessed other than by the now unproven theories which remain?

Juran & Schlosser (1978) increased their tensile strength estimates by employing a quasi-upper-bound calculation. Fig. 4(a) shows their typical method. They sought to determine which reinforcement first reaches its ultimate tensile strength by supposing that sufficient strain is permitted to enable a soil slippage to occur on some surface AC on which the angle of shearing resistance ϕ' is being developed. To enhance the strength beyond that predicted following the method of Fig. 2 they then constrained the available mechanisms by drawing a parallel between reinforced earth and braced cuttings: 'Therefore at failure, the only motion that is admitted to the upper part of the active zone is a vertical translation and the failure surface . . . must be orthogonal to the embankment free surface.' They correctly infer that for dilating soil the form of surface AC which would allow their active zone ABC to rotate as a rigid body is that of a logarithmic spiral. Unfortunately they chose the spiral shown in Fig. 4(a) which has an intrinsic angle ϕ', and whose pole O subtends angle OCB = ϕ'. They insisted that the tangent to the spiral at C should be vertical. Lord (1969) shows that this is an incorrect designation for a spiral intended to prevent lateral movement at B and C. Fig. 4(b) shows that the tangent to a spiral with an intrinsic angle ν must make the angle ν with the normal to BD at C if the velocity vector at C is to lie along that normal. If Juran & Schlosser had satisfied their own kinematical requirement, therefore, their spiral should have taken the form shown in Fig. 4(b). Neither is it necessary to adopt an artificial angle of dilatancy $\nu = \phi'$. It is possible to achieve solutions with the intrinsic angle of the spiral—perhaps $\nu = 20°$ for a dense sand in which $\phi' = 45°$—taking typical values from Roscoe (1970).

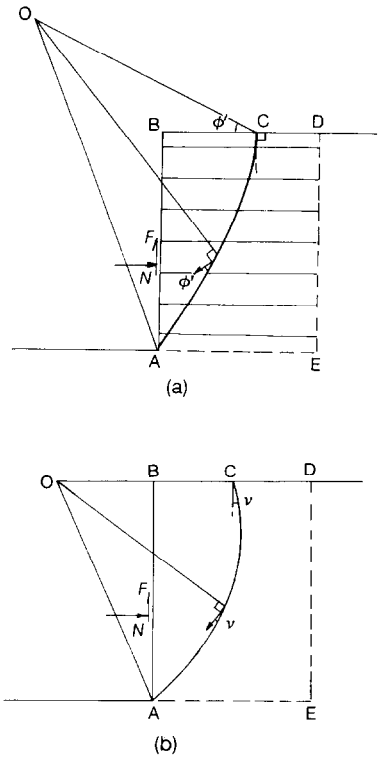

Fig. 4. Logarithmic spirals for restrained active walls: (a) ϕ' spiral (after Juran & Schlosser, 1978); (b) ν spiral (after Lord, 1969)

Even when the analysis of Juran & Schlosser is repeated with a consistent designation of logarithmic spiral, it is difficult to select which of the infinite number of available spirals is to be preferred. Each spiral generates its own equilibrium boundary forces F and N which must be carried partly into the reinforcement and partly into the facing footing at A. Further assumptions are necessary: Juran & Schlosser suppose that shear stresses are zero on horizontal planes in the active zone, although this seems to conflict with the generation of a large shear force F on the complementary vertical plane AB. This shear force is vital to their calculations because they note that in its absence the prediction degrades to that obtained in the simpler methods of Fig. 2. The final result is closely geared to the empirical production of an apparent earth pressure coefficient which is of the order of K_0 in the upper half of the structure and which drops below K_a in the lower half, while roughly maintaining the same overall active thrust at its Rankine value which can be derived from Fig. 2, and a slip surface which mirrors the data of the location of maximum tensions in the reinforcement of instrumented full-scale structures.

Against the background of inconsistencies and assumptions, it appears that the best justification for the method of Juran & Schlosser is its capability for fitting what they took to be relevant evidence. The centrifugal model data introduced now should demonstrate that these reactions to the strength underprediction problem may not be helpful because the evidence may not be relevant.

Mark I centrifugal model tests

Bolton *et al.* (1978) reported results obtained with a centrifuge package which could accelerate a model reinforced earth wall 200 mm high on a 60 mm deep sand foundation up to roughly 1300 m/s^2 or 130 g where g is earth's gravity. The width to height ratio of the models was never less than 2 so that plane strain behaviour of the central section was expected and observed. The ratio of reinforcement length to wall height L/H lay between 1·5 and 0·5. All the soil in the model, whether in the foundation, the reinforced zone or the backfill, was a dry, well-graded, natural sand placed by free fall from a hopper at a relative density of about 70% and a natural unit weight of 16·9 kN/m^3. The flexible, plane, foil facing was punched or slit at regular intervals to receive a uniform array of ties. The ties were of four sorts: copper-coated mild steel welding rod 1·5 mm in diameter (MS), stainless steel strip 6 mm wide and normally 0·1 mm thick (SS), aluminium foil normally 7·5 mm wide and 0·05 mm thick (AL), and the same aluminium foil coated with a silicone rubber called M-coat (ALM). Only one series of models was well instrumented with strain gauges and these were always extremely remote from tension failure ($F_T = 8·6$), although fairly close to slipping ($F_F = 1·29$). The main aim of this work (Choudhury, 1977) was to create a variety of collapses due to rupture or slippage of the ties.

Subsequent work has increased the number of model tests using this package, and slightly modified the friction parameters which represent the major uncertainty for the back analysis. Table 1 records the average peak values of ϕ' for the sand and μ for the various interfaces tested at an appropriate initial density in direct shear under a range of normal stresses in a 60 mm square shear box, and using the conventional assumption that ϕ' or μ as appropriate would be developed on the horizontal plane.

The philosophy underlying centrifugal testing has been discussed by Schofield (1980). The justification for performing centrifuge tests rather than simpler conventional model tests of reinforced earth walls lies chiefly in the facts that

(*a*) by creating an equality of stress in the model with that in a typical field-scale wall, the proper dilatancy of the soil is reflected; the sand in conventional small models dilates extremely strongly, and this must distort failure mechanisms
(*b*) by enhancing soil stresses, the requirements for the reinforcement are similarly increased, so that the additional stiffness created by strain gauges and lead wires is insignificant for the already substantial ties
(*c*) because the materials are thicker, the strength of the joints can be more easily controlled and the impact of local imperfections is reduced.

The main consistent errors implicit in centrifugal testing are due to the non-uniform acceleration field. The models described here are sufficiently small for the curvature of the field, with an effective radius of 1·5 m on the machine at the University of Manchester Institute of Science and Technology, to be ignored. The implied tilt of the crest of the wall $1/N$ is also negligible for tests when the enhancement factor N exceeds 30, which is the majority. The more serious error arises because the magnitude of the field at a point is proportional to the radius from that point to the axis of centrifugal rotation. The characteristic radius R_m of the present models was chosen to be at the mid-height of the wall, so that the characteristic enhancement factor N was $\omega^2 R_m/g$ at an angular velocity ω. This choice causes the stresses at the base of the wall to be correctly reproduced; those at the top of the wall are 7% less than those which would be observed in a geometrically similar field-scale wall N times higher. It is as though the soil at shallow depths were 7% less dense, although with unchanged

Table 1. Assumed friction properties of centrifugal models

Vertical stress σ_v: kN/m^2	Acceleration for σ_v at base: g	Sand		μ at interface			
		ϕ'	K_a	Sand and AL	Sand and MS*	Sand and SS	Sand and M-coat
50	15	49	0·140	0·36	0·33	0·18	0·70
100	30	47	0·155	0·56	0·33	0·17	0·72
200	60	45	0·172	0·60	0·33	0·16	0·75
400	120	43	0·189	0·65	0·33	0·16	0·75

* Artificial value of μ^* deduced from pull-out tests on these 1·5 mm dia. rods; $Q = (\pi BL)\mu^* \gamma Z$.

stress–strain characteristics. The main random errors arise from variations of $\pm 5\%$ in the relative density of the sand, implying $\pm 5\%$ in K_a, the strength of the ties ($\pm 6\%$, up to $\pm 10\%$ for the weakest), and the coefficient of friction of the ties against the soil ($\pm 5\%$, up to $\pm 10\%$ for the MS bars).

In order to test the adequacy of the friction criterion of equation (8), the calculated friction safety factor F_F is compared in Fig. 5 with the ideal value of unity in those cases where mark I models collapsed without there being any suspicion of breakdown in the reinforcement or facing. The centrifugal factor N at collapse is used on the ordinate to separate the results. The calculated F_F is shown for the most critical tie (i.e. that with the lowest value), which in each test corresponded to the deepest of the ten layers of reinforcement ($Z = 0{\cdot}190$ m). The only information used in the calculation was the fixed geometry of the model, the magnitude of the enhanced self-weight at the instant of collapse and the information stored in Table 1. The calculated value of F_F for models known to possess $F_F = 1$ varies from 0·97 to 1·30, with 11 out of 15 values lying in the range 0·97–1·07. The most erroneous value pertains to test C53, which was the sole example of a slippage of the aluminium foil reinforcement with the most variable coefficient of friction.

Many models were tested which did not collapse due to an insufficiency of friction. Two models with SS ties withstood maximum acceleration with F_F values of 1·01 and 0·97, these being the smallest values observed in models which did not collapse. Their deformations were relatively great, however, and they were judged to be on the point of collapse.

Figure 5 appears to confirm the adequacy of the criterion for F_F in equation (5) derived from simple stress analysis, especially with regard to organizing the data from a wide range of model types. A small degree of pessimism in the selection of values for the parameters in equation (8) would have conferred a sufficient degree of conservatism to prevent collapse. If, rather than taking average values for K_a and μ, the lowest values recorded in the shear box tests on the sand placed in the same fashion as in the model test had been chosen, the calculated values for F_F would have been lower by a factor of about 1·15. The residual overestimate would then have been no more than 1·15 in any case.

Figure 6 presents data of collapse attributed to tensile fracture of the reinforcement in the mark I models. At first sight there is even less cause for concern than with the data of friction failures because the worst overprediction from the 13 collapses was only by a factor 1·06 in test C52, which is well within the specified likely error band. However, the scatter is greater—0·50–1·06—and there is every indication that a substantial safety margin not introduced in equation (5) has been present in some of the models.

Models C51, C52 and C54 clearly did not possess this extra margin of safety. These had two common characteristics: they had relatively narrow configurations ($L/H = 0{\cdot}5$), and possessed the lowest friction factors F_F of the tension failure

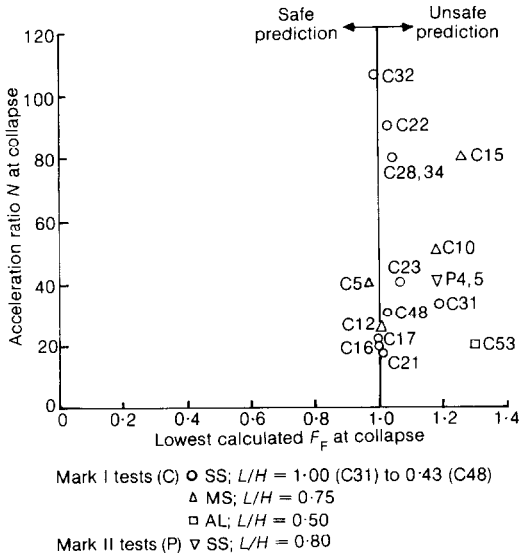

Fig. 5. Friction failures of walls with flexible facing

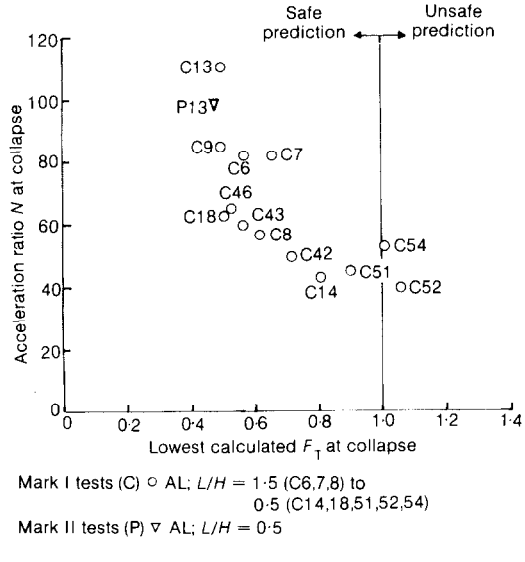

Fig. 6. Tension failures of walls with flexible facing

models. Indeed their friction capacity was nominally identical to that of model C53 which collapsed by slippage at $20g$.

A suitable hypothesis therefore would correlate the latent superiority of some of the models with an ability to redistribute tie forces in a way which would not be available if slippage failure were already imminent. An alternative hypothesis would centre on the possible effect of narrow configurations causing stress concentrations due to the overturning moments which were even harsher than those allowed for in equation (1). A third hypothesis would attribute the scatter to an undiscovered variation in the composition of the models. These issues were explored using a more heavily instrumented test package.

Mark II centrifugal model tests

A mark II test package, shown in Fig. 7 and described by Pang (1979), used the same sand and factory-trimmed aluminium reinforcement in a sequence of tightly controlled tests in which measurements were made of tie tensions at various locations, the vertical stresses beneath the reinforced zone and the boundary movements of the central plane. The 202 mm high model walls were built over a strong wooden foundation and confined between hard end walls which had been coated with a PTFE spray. Models were constructed in a similar fashion, but the facing usually comprised relatively stiff, articulated aluminium panels in contrast to the foil facing used previously.

A boundary pressure transducer, in the form of a simply supported beam, was specially developed to determine the vertical component of the contact stresses against the stiff foundation provided for these tests. The configuration (100 mm × 10 mm) of the transducer was chosen so that the presumably steep stress gradient near the face of the wall would be averaged over only 10 mm, and the length of 100 mm was small enough to guarantee that the central deflexion of the beam could be kept below 10^{-2} mm in all circumstances. The theoretical calibration of these devices corresponded quite well with dead weight tests, which in turn agreed within 3% with a centrifugal calibration under sand, showing that the soil–structure stiffness ratio of the beam was sufficiently small. The readings could be expected to be accurate to within ±10% of their proper value.

The reinforcing strips were subjected to strength tests and those which were strain-gauged were also individually calibrated by the application of dead weights. Fig. 8 shows a typical stress–strain curve to rupture which was selected from eight tests on a batch of strips. The initial elastic response with a gradient $E = 63\,000$ N/mm^2 led to a first yield at

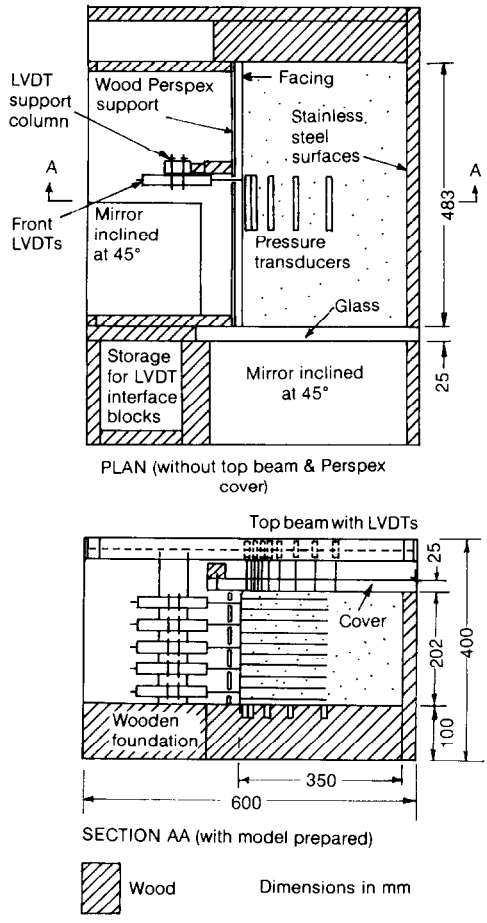

Fig. 7. Mark II model package (excluding steel container)

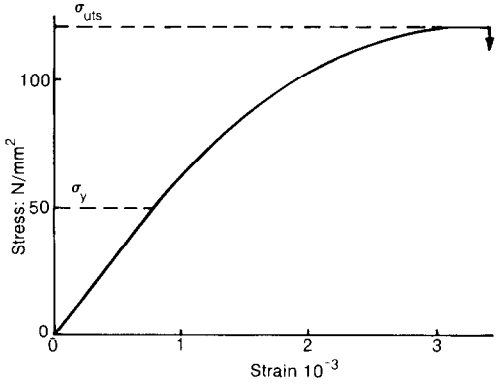

Fig. 8. Tensile test to rupture on an aluminium strip (160 mm × 4 mm + 0·1 mm)

Table 2. Test data from mark II package, $H = 202$ mm

Test	Facing*	Reinforcement details						Critical conditions					
		Type†	L: mm	B: mm	S_v: mm	S_h: mm	P: kgf	μ	K_a	F_F§	F_T§	N_{max}	Collapse mode
4	F	SS	160	6	20	70	87	0·17	0·160	1·19	23·1	42	F
5	F	SS	160	6	20	70	87	0·17	0·160	1·19	23·1	40	F
13	F	AL, M	100	4	20	40	3·8	0·75	0·186	2·41	0·48	98	T
6	P	AL	160	4	20	80	4·8	0·65	0·183	2·47	0·47	92	T
7, 8	P	AL	160	4	20	80	4·8	0·60	0·172	2·43	0·74	63	—
9	P	AL	160	4	20	80	4·8	0·60	0·172	2·43	0·74	63	T
10	P	AL	160	4	20	80	4·8	0·61	0·176	2·41	0·65	70	T
14	P	AL, M	160	4	20	80	5·1	0·73	0·165	3·08	1·12	46	—
20	P	AL, M	100	4	20	80	5·1	0·75	0·180	1·81	0·55	85	T
11	P	AL, M	100	4	20	40	3·8	0·75	0·189	3·45	0·53	125	—
12	P	AL, M	100	4	20	40	3·8	0·75	0·189	3·45	0·56	119	T
16	S	AL, M	100	4	50	20	3·8	0·75	0·189	2·76	0·43	125	—
17	P	AL, M	100	4	20	40	5·1	0·75	0·176	3·71	1·36	71	—
19	P	AL, M	100	4	20	40	5·1	0·74	0·165	3·90	2·09	49	—
21	P	SS, M	160	4	20	40	26	0·74	0·165	6·2	10·6	49	—

* F flexible aluminium foil, 0·15 mm; P stiffer aluminium panels, 1 mm, articulated; S single aluminium sheet, 1 mm.

† SS stainless steel; AL aluminium; M coated with M-coat.

§ Limit factors calculated for most critical strand at N_{max}, using $F_F = 2BL\mu/S_v S_h K_a F_v$ and $F_T = P/K_a \gamma Z S_v S_h F_v$, where F_v is an estimate of the enhancement of vertical stress at the facing which has been taken to be $(1 + K_a Z^2/L^2)$ for models with flexible facing and 1·15 for all models with stiffer facing, using data of Fig. 9, and where the self-weight of the soil γ is $16{\cdot}9\, N_{max}$ kN/m^3.

‖ F friction failure, slippage; T tension failure, rupture.

$\sigma_y = 50\,N/mm^2$, followed by strain hardening to rupture at a tensile strength $\sigma_{uts} = 118\,N/mm^2$, with a strain at rupture of only 0·35% of the length of the test piece. This limited ductility of the 4 mm × 0·1 mm foil strip was thought to place the model ties in roughly the same category as full-scale mild steel or aluminium strip with weak joints or localized corrosion, as it represented the equivalent of 30% elongation to rupture over a 50 mm long critical section on a typical 4 m long strip of reinforcement.

In order to be able to assign a reliable stress to the strain gauge readings beyond the elastic range it was necessary to take a number of gauged strips to destruction. The form of the strain hardening curve was sufficiently stable to imply that the error was no greater than about ±5% when the initial gradient and yield point were used to normalize the higher readings from the 4 mm × 0·1 mm strips. The thinner 4 mm × 0·05 mm strips were subject to ±8% variation in their rupture strengths.

Table 2 gives the statistics of a group of tests on

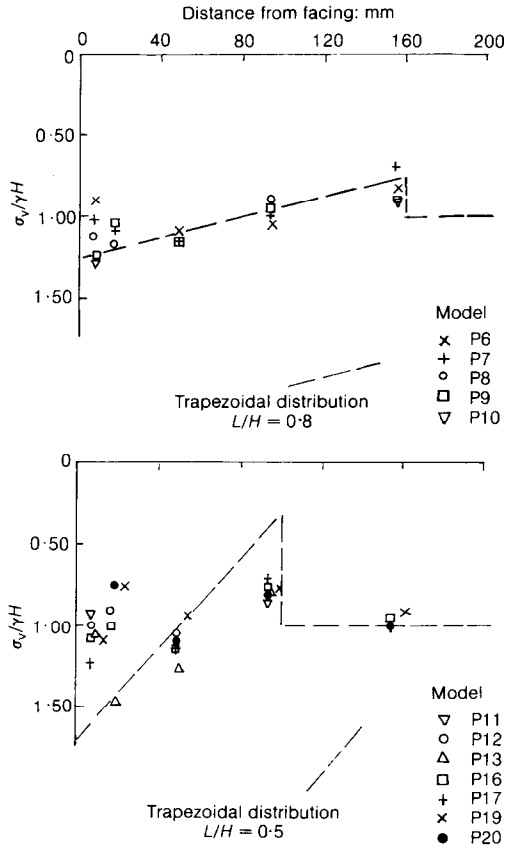

Fig. 9. Vertical stress distributions at the base of mark II model walls (model P13 foil facing; others panel facing)

models using the mark II package. The presence of base pressure cells meant that the previous assumption of a trapezoidal distribution of vertical stress could be abandoned in favour of the measurements. Fig. 9 shows the distributions which were obtained. The increase in the output of any particular cell was characteristically in proportion to the applied increase in the self-weight of the soil, so that in Fig. 9 all the data from a cell can be represented by a single point indicating the ratio by which its recorded pressure exceeded the simple overburden pressure.

The trapezoidal distribution of equation (1) would always have provided a conservative estimate of the vertical soil stress behind the facing panels. When the facing was a relatively flexible 0·15 mm foil, as in test P13, the maximum vertical stress ratio $\sigma_v/\gamma H$ occurred 20 mm behind the facing and was found to be 1·48, compared with the trapezoidal estimate of 1·75 for a wall with $L/H = 0{\cdot}5$. When the facing was a single relatively stiff 1 mm sheet, as in test P16, or a group of 1 mm thick articulated panels, as in test P17, the maximum vertical stress ratio for the same narrow configuration was typically 1·15. The wider walls with $L/H = 0{\cdot}8$ behaved more in conformity with the trapezoidal rule, although 1·15 was again a more characteristic maximum enhancement factor for these models with stiff facing than the factor of 1·25 given by equation (1).

In each case there seems to be a zone directly behind the facing in which the vertical stress varies incoherently between its maximum value and unity (or less). This evidence should be coupled with the marked overall reduction in vertical soil stress when stiff rather than flexible facing panels are used. A suitable hypothesis is

(*a*) stiff articulated facing panels can develop substantial shear stresses on their buried surfaces

(*b*) the magnitude of these shear stresses is variable, depending on the minutiae of relative vertical displacements, including those due to the closing of the irregular gaps between panels

(*c*) that where stiff panels are supported at their base by a stiff foundation, the thrust accumulated in a stack of panels can be sufficient to reduce the vertical soil stresses over a wide area, and by as much as 25% in the region of greatest stress.

The data of the collapse of the flexibly faced models P4 and P5 in the mark II package are compared in Fig. 5 with those of models similar to C23 in the mark I package which were also flexibly faced and failed due to lack of friction. The slight changes in boundary conditions and preparation procedure adopted in the mark II models have

evidently not affected their behaviour relative to those already described. However, it is evident from Fig. 6 that the scatter in the data of tension failures in the flexibly faced mark I models have simply been confirmed by the data of mark II model P13. This collapsed at 98 g when F_T was calculated to be 0·48, whereas model C54, which possessed the same aspect ratio and an almost identical distribution of reinforcement strengths, had collapsed at 53 g when F_T was calculated to be 1·01. Such large discrepancies in the results of almost identical models cannot be due to the algebra of equation (5), but rather to the presence of previously undiscovered differences between apparently similar models.

The key to the solution of the problem may be found in the results of tests on models P6, P7, P8, P9 and P10 which were nominally identical (Table 2). The range of accelerations to collapse was 63–92 g, although models P8 and P9 were deliberately left intact. Fig. 9 shows that the vertical soil stresses under these walls were similar to within $\pm 10\%$, except within 20 mm of the facing where the apparent variation was $\pm 20\%$. Fig. 10 shows that up to an acceleration of 63 g the tensile forces derived from strain gauges at various positions in the five models could be superimposed with little scatter. The shape of the distribution of peak tension, which occurred 30–40 mm behind the facing, remained constant up to this acceleration in these tests.

Figure 11 compares the peak values at various depths with a simple active anchor estimate made using equation (4). Peak tensions follow the prediction quite well in the upper three quarters of the model. However, the tests showed that, instead of providing greatest tensions in the bottom layer of reinforcement, the layer 150 mm down the 200 mm wall is critical.

Although the data of the models could be amalgamated up to an acceleration of 63 g, this was not possible thereafter. Fig. 12 shows some data of peak tensile forces inferred in strands of reinforcement at the critical depth of 150 mm in models P8, P9 and P10. In model P8 at 63 g the

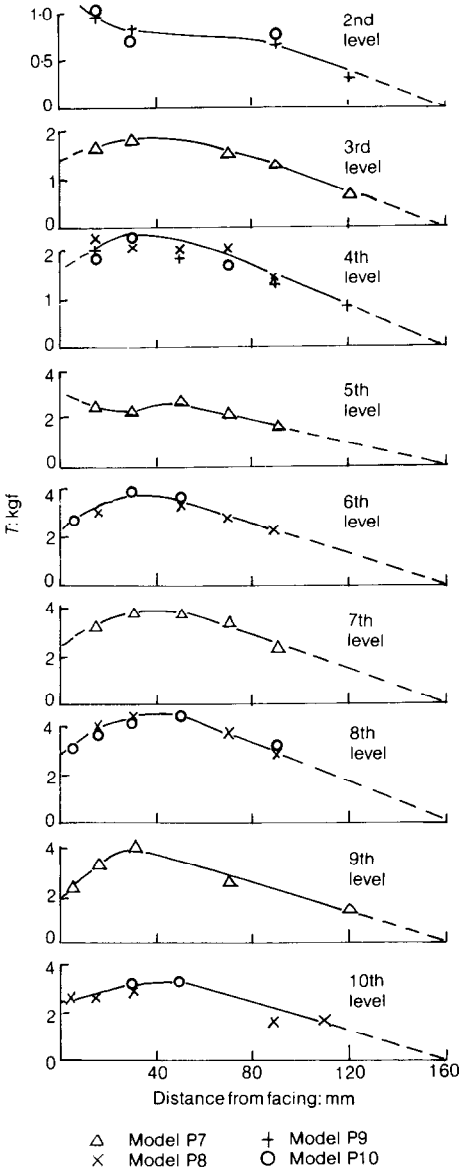

Fig. 10. Merged tension distributions from models P7, P8, P9 and P10 at 63 g

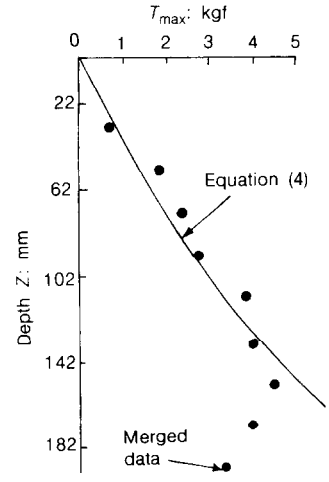

Fig. 11. Peak tensions at 63 g in models P7, P8, P9 and P10

gauge 30 mm from the facing showed that the parent tie was approaching its nominal tensile strength at that position. In model P9 at 63 g the same gauge showed that the tie had effectively reached its tensile strength, but an earlier event was also of interest. A gauge on another tie and 5 mm from the facing had broken at 30 g. This was attributed to the weakening of the local joint caused by the repeated use of strips in the sequence of models, associated with bending during each manufacture.

For model P10, with fresh strips in the critical positions, at 63 g the ties with gauges at 30 mm and 50 mm had effectively reached their nominal tensile strength at these positions. The sharp fall after 63 g in the signals from gauges at 5 mm and 15 mm on other ties at this level can best be interpreted in the light of the evidence of the subsequent post-collapse investigation in that ruptures had occurred in these ties at distances of 28 mm and 38 mm from the facing. It may be supposed that the full tensile strength of these strips had also been mobilized at 63 g.

It becomes clear that in these models the first ties to reach their tensile strength do so at 63 g; they lie at a depth $Z \simeq 0{\cdot}75H$ and their critical position is a distance $X \simeq 0{\cdot}15H$ inside the facing. If, as in the model P9, there is a small flaw in the pattern of reinforcement the model will be likely to withstand no more. If, in the absence of such flaws, the mobilization of the tensile strength of these ties at 63 g is followed by a pattern of strains which progressively cause ruptures in the relatively brittle strips, the model cannot be expected to show much more than the 10% capacity for overload enjoyed by model P10. The extra capacity of model P6, which lasted up to 92 g, must therefore indicate that plastic strains permitted a redistribution of extra stresses around the critical zone so that the reinforcement therein could maintain its peak tension at its tensile strength while the self-weight of the model increased by a further 46%.

The conservative nature of equation (5) when used to predict the collapse of a reinforced earth retaining wall is now clarified with respect to the walls which had an aspect ratio $L/H = 0{\cdot}8$. In particular, one source of strength underprediction seems to be an ability at all stages to arch stresses away from the reinforcement in the zone behind the facing in the lower quarter of the wall. This creates an extra margin of safety of about 1·4, in the sense that when the tensile strength of a tie is first reached, the simple anchor theory of equation (5) would have said that the safety factor of a tie in the lowest layer was 1/1·4. The roots of this behaviour must lie mainly in friction against the foundation which will tend to prevent the outward movement of the lowest facing panel and the sand behind it, and also the friction against the back of the facing which will tend to reduce the vertical stresses in the soil behind the facing. This factor can presumably be reduced to unity if the facing is either perfectly smooth or perfectly flexible in the vertical plane, and if the foundation contains relatively weak strata.

Another source of strength underprediction is an ability to tolerate the growth of a plastic zone in which the reinforcement has approached its tensile strength while the load carrying capacity of the construction as a whole is increased by a factor of up to 1·5 following redistributions of stress increments to zones of the structure which can still accommodate them. This factor can presumably

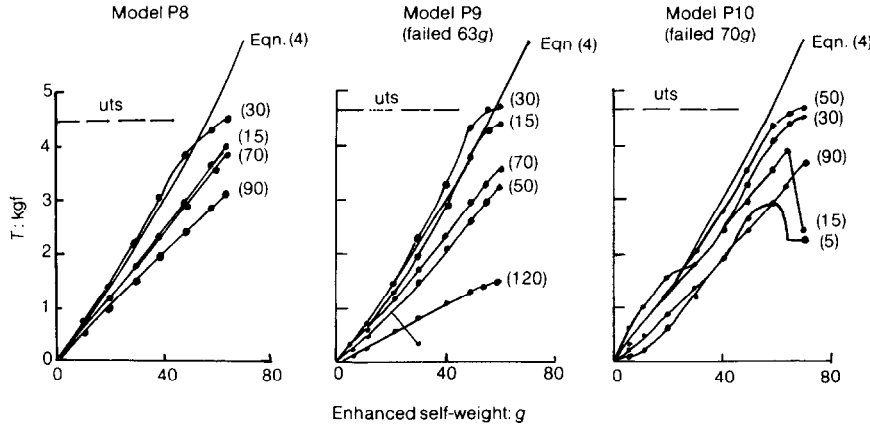

Fig. 12. Critical tension measurements at 150 mm depth in nominally identical models

be reduced to unity if the reinforcement is extremely brittle, or if the soil strength is completely mobilized in preventing slippage.

Further evidence of the progress towards tensile collapse was collected during test P20 on a narrow wall with $L/H = 0{\cdot}5$. Fig. 13 shows that the peak tension in the lower third of the wall increased almost uniformly from zero and came to tensile strength roughly simultaneously at an acceleration of about $72g$ before the wall collapsed completely at $85g$. In this case the arching factor is evidently 2·2; this is made up of a factor of about 1·6 attributable to the vertical stresses behind the facing, which were shown in Fig. 9 to be reduced by roughly this amount compared with the trapezoidal estimate, and a further factor of 1·4 which must represent the friction of the lowest facing panel against the foundation. The plastic redistribution factor was 1·2 in this case.

The mark II models discussed so far were each reinforced in such a way that the strips possessed a safety factor against slippage F_F of less than 2 for at least part of their progress towards tensile rupture. Models P11, P12, P17 and P19 were nominally identical in their greater friction capacity, having a value of F_F of about 3·5 at all stages of testing. The vertical stresses under the bases of these narrow models ($L/H = 0{\cdot}5$) are shown in Fig. 9 to have been similar to those of model P20. It is perhaps not surprising, therefore, that the calculated tensile safety factors F_T of the lowest ties at the instant of collapse in models P20 and P12 were almost identical, whereas model P11 which had a slightly stiffer facing system was able to develop a small margin of extra strength sufficient to take it outside the capacity of the centrifuge to destroy it, although deformation measurements indicated that collapse was probably imminent. Evidently the virtual doubling of friction capacity does little or nothing to alter the combined value of the arching factor and the plastic re-distribution factor at collapse.

However, the enhanced strip friction has a significant effect on the development of tensile forces before collapse. Fig. 14 compares the peak tensions developed in the two configurations, using a mobilized earth pressure coefficient $K_m = T_{max}/\gamma Z S_v S_h$ derived by analogy with equation (4). The trapezoidal enhancement factor has been omitted on the grounds that Fig. 9 has shown that the vertical stresses at the base are only in the vicinity γZ. The peak tension T_{max} has been divided by $S_v S_h$ on the presumption that this ratio will approximate to the lateral stress in the zone of peak tension.

It is evident that the arrangement with greater friction capacity in models P17 and P19 led to the creation of relatively greater earth pressures in the early stages. The larger coefficient $K_0 = 1 - \sin\phi'$ is a better empirical guide to these initial reinforcement tensions than the active earth pressure coefficient K_a. However, the condition of collapse of the originally identical model P12 has shown that even the coefficient K_a is a pessimistic predictor, unless account is taken of possible arching and plastic stress redistribution.

Ideally structures should not collapse without

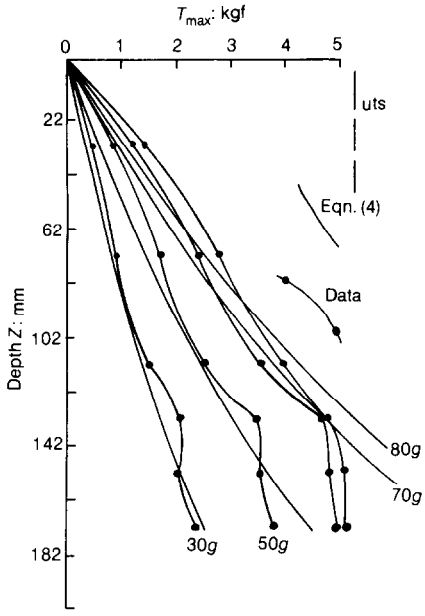

Fig. 13. Peak tensions in model P20, $L/H = 0{\cdot}5$, collapsed at $85g$

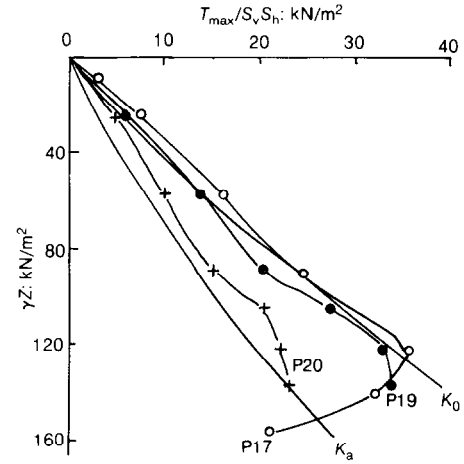

Fig. 14. Earth pressures mobilized at $50g$ in models remote from tensile failure; frictional capacity of models P17 and P19 is double that of P20

warning. The boundary displacements of the mark II models were measured by displacement transducers with the aim of determining whether or not collapse could be predicted in this way. The lateral crest deflexions in Fig. 15 show that a point of inflexion usually occurred at a load factor to failure of about 1·4, often correlating with the first approach to the tensile strength of the reinforcement. The distortion (i.e. crest deflexion divided by wall height) at collapse was only about 1/60 for most of the models; it was largest—1/30—in test P13 on a narrow wall with flexible facing. The magnitude of the increase in the rate of deflexion from a load factor of 1·4 to failure is therefore not such as to make it likely that it would be noted at field scale, in view of the erratic application of loads.

CHOICE OF ANALYSIS

Many research workers and design authorities have assumed that the rupture of the first strand of reinforcement in tension will generate and coincide

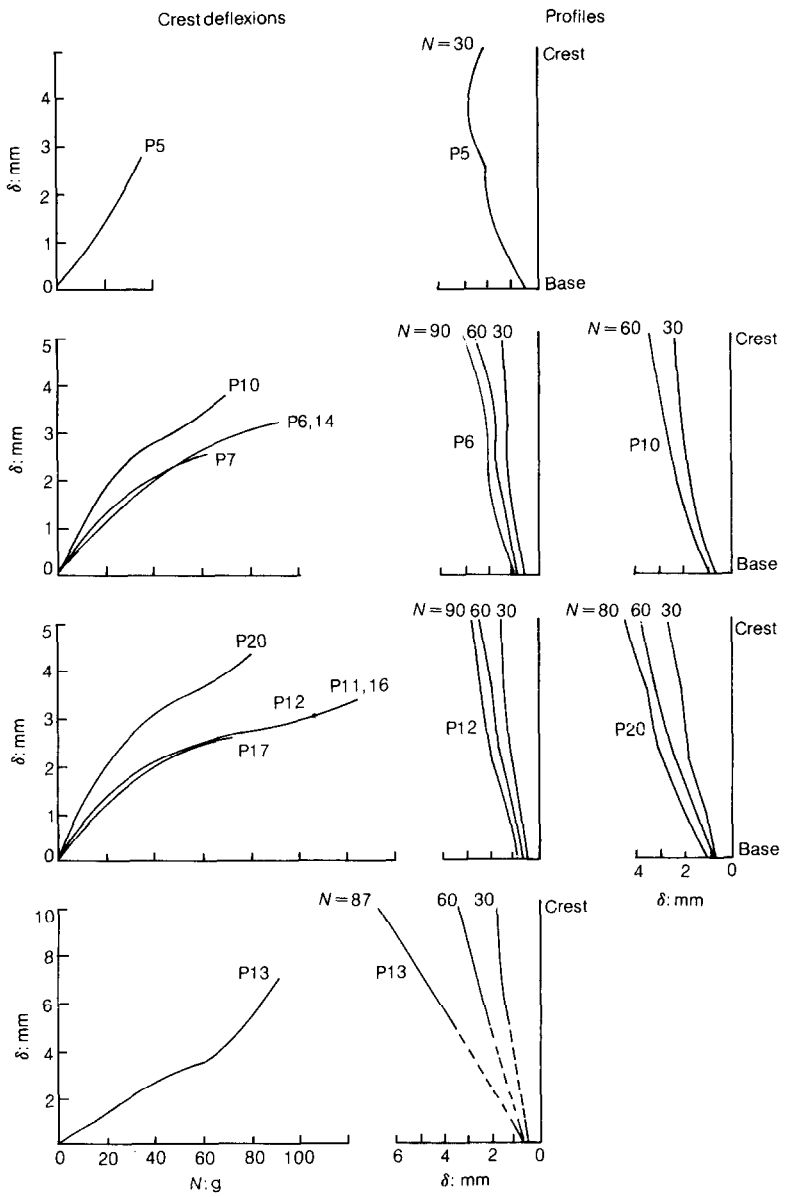

Fig. 15. Forward deflexions of the model faces

with the collapse of the whole reinforced earth construction. Tension data such as those in Fig. 12 have shown that this is not necessarily the case. Although the models used to create the data were constructed with reinforcing strips which elongate very little to rupture, a similar lack of overall ductility would be found if a full-scale trial were made of a strip which had suffered localized loss of area due to corrosion of the presence of bolted connections. Two of the conditions specified by the Institution of Structural Engineers (1955) ((*b*) and (*c*) in the section on design requirements) appear to require the redefinition of the tension limit itself, such that no strand of reinforcement shall approach its ultimate tensile strength under any foreseeable conditions. This would imply that designers should not attempt to use stress redistribution among reinforcing elements carrying their full tensile strength, notwithstanding the fact that this phenomenon increases failure loads in tension by factors of up to 1·5.

It follows that all previous model or field tests to collapse which relied on the back-analysis of a tension failure to test a collapse limit expression are unreliable. It is necessary to measure the distribution of reinforcement tensions in order to capture the first approach to full tensile strength at any location. This technique in the centrifuge models has also shown the error of using the positions of strip rupture in any back-analysis. Whereas peak tensions in the instant before collapse were typically developed in a vertical plane 30 mm behind the facing, the tie ruptures were only in this region at the point from which collapse began. Above and below the critical zone the ruptures often occurred at the facing joints or along the hypotenuse of an active triangle. These dynamic effects are not significant to the designer.

A phenomenon called arching has been seen to reduce reinforcement tensions in the lowest quarter of the walls, compared with equation (4). At the base of the walls the reduction factors are about 1·4 for all walls with a conventional aspect ratio ($L/H = 0{\cdot}8$), 1·7 for narrow ($L/H = 0{\cdot}5$) walls with flexible facing sheets which could easily buckle under an accumulated vertical thrust, and 2·2 for narrow walls with stiff facing panels. However, existing model and field tests to collapse are inadequate for safely enhancing the simple limit factor of equation (5) by the further adjustments which would deal with arching of stresses and forces in a practical case. The value of the centrifugal model tests is that they suggest that any detail such as the presence of plastic foam to prevent dirt washing out of the joints between facing panels, the pragmatic placement and subsequent removal of wooden wedges in the joints to achieve stated tolerances, the presence of a soft clayey stratum in the foundation soil, the sequence of placement of the backfill over compressive foundation soils, or the effects of future mining subsidence, is likely to alter significantly the degree of arching which will supplement the simple anchor behaviour of equation (5). However, there is no suggestion from the present data that the simple analysis will ever be unsafe on these grounds, and so the method has everything to recommend it to a designer.

The criterion for collapse by slippage represented by equation (8) was fairly accurate in the back-analysis in Fig. 5, so that it may seem unnecessary to alter it. However, the evidence from tests on models with $F_F < 2$, which includes the small stress results of P7, P8, P9 and P10 and tests C19, C20, C27 and C33, all of which had $L/H = 0{\cdot}8$, and P20 which had $L/H = 0{\cdot}5$, was that peak tensions developed at about 30 mm from the facing of these 200 mm high walls. It may therefore be prudent to reduce the effective anchor length to $L' = L - 0{\cdot}15H$ so as to account for the lack of observation of supportive shear stresses in the foremost zone of the reinforcements and for the unexplained marginal optimism in Fig. 5. The modified formula is then

$$F_F = \frac{2B(L - 0{\cdot}15H)}{S_v S_h K_a (1 + K_a Z^2/L^2)} \tag{9}$$

which would have predicted a minimum friction safety factor for anchors in models which failed by slippage in the range 0·67–1·01. This is entirely consistent with knowledge of the effect of arching. It would appear to be unnecessary to develop other formulae corresponding to the supposed creation of rupture surfaces.

The stress analysis following Fig. 3 has been shown to be necessary in the prevention of tensile limit states, and it is useful as a basis for the prevention of friction limit states. It can also provide a convenient approach to the elimination of monolithic collapses as the normal and shear stresses on the base can be compared directly with those which might be considered limiting from the viewpoint of a foundation calculation. A consistent approach can therefore be adopted throughout the exercise of avoiding limiting conditions within and around the surface of a reinforced soil mass.

The only significant obstacle to this approach is the modification to the simple self-weight problem caused by the possible imposition of concentrated surface loads. This problem affects the design of every type of retaining wall and, in the absence of data on collapse caused by concentrated loads, it can be tackled only on the basis of an assumed stress distribution which it is hoped will be pessimistic. Whereas wall designers have been able

to use such mechanistic analyses as the trial wedge method for the design of unreinforced fills subject to line loads, the centrifuge tests reported here suggest that this will not be satisfactory in the case of reinforced fills. If the relatively benign stress gradients caused by self-weight have been able to promote localized ruptures and progressive collapse, it must be anticipated that concentrated loads may similarly generate localized and progressive failures which can be forestalled only by stress analysis.

SELECTION OF MATERIALS AND APPROPRIATE VALUES FOR PARAMETERS

The keys to an assessment of the strength of a well-drained reinforced earth retaining wall have been found to be the friction parameters K_a and μ, and the tensile strength P of the anchors. Most investigators have discovered that reinforcements in field structures develop tensions in proportion to K_0 rather than K_a, and have attributed this to compaction stresses. It is clear that compaction may have a dominant effect in establishing the state of stress in a body of earth at rest, but measurements on the centrifugal models which were remote from failure also showed tensions proportional to K_0, even though no compaction loads had been applied. As these models approached collapse it was shown that the effective earth pressure coefficient dropped to K_a. At collapse the same models often showed further self-supporting tendencies, which made even the simple active predictions a little conservative. It may be inferred that a similar process would occur in the field, and that the measurement in a sound structure of at-rest lateral pressures greater than the active assumption should not undermine the confidence of the designer in the active limit state calculations.

The proper values for the parameters K_a, μ and P should be determined on the evidence of laboratory tests on the materials and in relation to a sequence of possible limit state scenarios. Extensive theoretical and experimental research testifies that the active earth pressure coefficient K_a for a granular soil in plane compression varies over its possible range of densities by a factor of 2:1. The higher value of K_a corresponds to loose soil which does not dilate on shearing, and which therefore tends to approach its critical state strength without exhibiting any prior peak in its stress–strain curves. The lower value for K_a relates to the temporary peak strength of dense dilatant soil: beyond the peak, the mobilized coefficient K_a rises to regain its critical state value when the boundary displacements have been such as to create a fully remoulded shear zone within the once homogeneous and dense soil skeleton.

Many reinforced earth walls will be founded on compressible soils or in regions subject to mining subsidence. Until evidence shows to the contrary, the designer of such structures should suppose that some pattern of base deformation might allow the formation of a sliding wedge of reinforced soil, as in Fig. 2(a), or a similar wedge in the retained backfill. Such a mechanism could cause softening in the zone of the active shear plane, leading to a rise in the earth pressure coefficient. When the inevitable uncertainty concerning the achievements of the field compaction process is also considered, it will be evident that the most sensible general course will be to invoke the critical state earth pressure coefficient, and therefore to design walls which can just tolerate the pressure of loose earth.

The selection of an appropriate value for the minimal tensile strength of a reinforcing element and its connection, especially regarding the possibility of long-term corrosion in the ground, is outside the scope of this Paper. However, there is an interaction between design decisions on joints and protection against corrosion and the likely limit state behaviour of the structure. Cole (1978) showed that the form of connection usually used for strip elements—a single dowel or a pair of bolts—is unlikely to display an efficiency of greater than 65% with respect to the strength of the parent strip. This is regrettable on the grounds of economy because the lower joint strength must be used in the tensile strength criterion (equation (5)). Care must also be taken to ensure that the overall ductility of the structure is not reduced too far. The fracture of a bolted or dowelled strip in tension usually occurs in the net or reduced section neighbouring the hole. The elongation to fracture would therefore be proportional only to the diameter of the hole rather than the length of the strip, unless the phenomenon of strain hardening could be relied on to so increase the strength of the connection that the gross section yielded before the net section at the connection broke. Fisher & Struik (1974) express this in the form of the yield requirement

$$\frac{\text{net cross-sectional area}}{\text{gross cross-sectional area}} \geqslant \frac{\text{yield stress}}{\text{tensile strength}}$$

which they apply routinely to the design of connections because 'it is usually considered desirable for the system to have capacity for distortion or geometrical adjustment before failure by fracture'.

The problems of protection against corrosion for metallic strips are perhaps more serious, because the simplest strategy of using coatings may not be available if the interfacial friction of the

strips is reduced. The next preferred strategy is to add a sacrificial layer of the parent material to each exposed surface. Unless the yield requirement is applied to the post-corrosion limit states, the resulting structure may not be able to react in a ductile fashion to future loads or ground displacement.

Suppose that some galvanizing treatment can be relied on to provide adequate protection to a low-carbon steel for a few decades, but that the requirement of a buried service life of over 100 years implies that a sacrificial layer of 0·75 mm will be necessary on each exposed surface. The sacrificial corrosion allowance would then be 1·5 mm on the thickness of each strand of reinforcement. The strength requirement of the reinforcement, which may be placed at small intervals in order to reduce the size of facing panels or to provide sufficient friction, might be only for strands 0·5 mm thick. The designer is then implying that it will be satisfactory to lose three quarters of the gross cross-sectional area of the strip in service. However, the details of the pattern of corrosion as it will develop will remain uncertain. If the loss of sacrificial material occurs only in a 100 mm length adjacent to the front joint, or beneath a leaking highway drain, the threat of local rupture in the absence of general yield is severe.

If the concept of sacrificial layers can be validated, there are strong grounds for applying the same yield requirement to the expected loss of material due to corrosion which was introduced to deal with the reduction of net area at joints. If the elongation to fracture were only of the order of 15 mm for a typical 4 m strip, as it might be if the fracture of a reduced section were permitted to occur before general yield, the overall degree of brittleness would be well modelled by the aluminium strips used in the centrifuge tests. Although this degree of brittleness can be tolerated if an elementary plastic stress analysis is carried out, progressive rupture could take place. Two of the conditions specified by the Institution of Structural Engineers (1955) ((*b*) and (*c*) in the section on design requirements) would forbid the use of a form of construction in which accidental overloads might leave the structure with certain hidden elements broken although the boundary displacements cause no apprehension. Since this degree of brittleness can be reduced, there are grounds for insisting that it should be.

The new yield condition may often require material such as galvanized mild steel to be avoided in zones of low stress where there is an expectation of significant corrosion. The relative merits and costs of stainless steels are discussed by Cole (1978) and Lee & Edwards (1978). The tensile properties of a quarter-hard, cold-rolled, stainless steel of type 316S16 might be roughly: ultimate tensile strength 850 N/mm^2, 0·2% proof stress 510 N/mm^2 and elongation 25%. The nominal sacrificial thickness might be a few tenths of a millimetre, which could make it possible to fulfil the yield requirement economically in most circumstances.

CONCLUSIONS

Insufficient attention has been paid by designers of reinforced earth to the requirement that adequate warning of danger be given by visible signs and that none of these signs shall be evident under design working loads. Imperfections lead to overall brittleness even in reinforcing elements made of ductile materials. Centrifuge model tests have indicated that such elements may rupture in various sequences and at various strains, so that the overall collapse load of the construction is uncertain. Reinforcing elements in the field are conventionally designed with weak joints and they will also suffer local deteriorations; they must therefore be expected to rupture at relatively small but unpredictable overall extensions. In these circumstances it appears to be justified to impose an overall yield condition on metallic reinforcement which will ensure that under an unexpected future overload the gross strip can yield plastically before the joint, or any corroded section, ruptures.

Centrifuge model tests have shown that it is necessary to revise the definition of the tensile limit state in reinforced earth structures. What matters is the first approach of a reinforcing element to its ultimate tensile strength. Plastic redistribution of forces around buried elements in this condition, although it has been seen to contribute up to an extra 50% of the load-carrying capacity of the structure, is too uncertain a source of strength when the elements may not have a reliably large extension to rupture. Upper-bound calculations using general collapse mechanisms automatically invoke plastic redistribution of forces, and are therefore not recommended.

Simple stress analysis after the fashion developed by Rankine has proved to be pessimistic in predicting the first mobilization of tensile strength in the model reinforcement. This degree of pessimism was associated partly with a reduction of stress at the toe of the wall due to wall friction, and partly with friction between the base of the wall panels and their foundation. Neither of these effects could be expected to be a reliable and predictable source of strength to the designer unless extraordinary measures were taken on site to control, for example, facing joint sealants and spacers. The simple analysis is therefore recommended for design.

ACKNOWLEDGEMENTS

The experimental work was conducted on the 100g tonne centrifugal testing facility in the Department of Civil Engineering at the University of Manchester Institute of Science and Technology. The Authors' thanks are due to Professor M. Burdekin and the staff of the Institute, in particular the technical staff, Mr L. Lardi and Mr A. Kirk.

The work was funded partly by the Transport and Road Research Laboratory, and partly by the Institute. The views expressed are solely those of the Authors and are not necessarily those of the Department of Transport or of the Transport and Road Research Laboratory.

REFERENCES

Al-Hussaini, M. & Perry, E. B. (1978). Field experiment of reinforced earth wall. *J. Geotech. Engng Div. Am. Soc. Civ. Engrs* **104**, GT 3, 307–322.

Bacot, J. & Lareal, P. (1979). Calcul de la hauteur critique de rupture des murs en terre armée d'après étude sur modèles réduites. In *Proceedings of international conference on soil reinforcement*, vol. 1, pp 17–22. Laboratoire Central des Ponts et Chaussées.

Banerjee, P. K. (1975). Principles of analysis and design of reinforced earth retaining walls. *Highw. Engr* **22**, No. 1, 13–18.

Binquet, J. & Carlier, C. (1973). *Etude expérimentale de la rupture de murs en terre armée sur modèle tridimensionnel.* Internal report. Laboratoire Central des Ponts et Chaussées.

Bolton, M. D., Choudhury, S. P. & Pang, P. L. R. (1978). Modelling reinforced earth. *Ground Engng* **11**, No. 6, 19–24.

Choudhury, S. P. (1977). *A study of reinforced earth retaining walls with sand backfill by centrifugal modelling.* PhD thesis, University of Manchester Institute of Science and Technology.

Cole, E. R. L. (1978). Design aspects of reinforced earth construction. *Ground Engng* **11**, No. 6, 49 52.

Finlay, T. W. & Sutherland, H. B. (1977). Field measurements on a reinforced earth wall at Granton. *Proc. 9th Int. Conf. Soil Mech., Tokyo* **1**, 511–516.

Fisher, J. W. & Struik, J. H. A. (1974). *Guide to design criteria for bolted and riveted joints*, pp. 100–105. New York: Wiley.

Institution of Structural Engineers (1955). Report on structural safety. *Struct. Engr* **33**, May, 141–149.

Juran, I. & Schlosser, F. (1978). Theoretical analysis of failure in reinforced earth structures. In *Proceedings of symposium on Earth Reinforcement*, pp 528–555. Pittsburgh: American Society of Civil Engineers.

Lee, B. V. & Edwards, A. M. (1979). The use of high alloy steels in resisting corrosion. In *Proceedings of symposium on reinforced earth and other composite soil techniques*, pp 286–292. Suppl. Report 457. Crowthorne: Transport and Road Research Laboratory.

Lee, K. L., Adams, B. D. & Vagneron, J. J. (1973). Reinforced earth retaining walls. *J. Soil Mech. Fdns Div. Am. Soc. Civ. Engrs* **99**, SM 10, 745–764.

Lord, J. A. (1969). *Stresses and strains in an earth pressure problem.* PhD thesis, University of Cambridge.

Luong, M. P. (1980). Stress–strain aspects of cohesionless soils under cyclic and transient loading. *International symposium on soils under cyclic and transient loading*, vol. 1, pp 315–324. University of Swansea.

Pang, P. L. R. (1979). *Centrifugal model tests of reinforced earth walls.* PhD thesis, University of Manchester Institute of Science and Technology.

Roscoe, K. H. (1970). The influence of strains in soil mechanics. *Géotechnique* **20**, No. 2, 129–170.

Schlosser, F. & Long, N. T. (1974). Recent results in French research on reinforced earth. *J. Construct. Div. Am. Soc. Civ. Engrs* **100**, CO 3, 223–237.

Schlosser, F. & Segrestin, P. (1979). Local stability analysis method of design of reinforced earth structures. In *Proceedings of international conference on soil reinforcement*, vol. 1, pp 157–162. Laboratoire Central des Ponts et Chaussées.

Schlosser, F. & Vidal, H. (1969). Reinforced earth. *Bull. Liais. Labs Ponts et Chaussées* **41**, 101–144.

Schofield, A. N. (1980). Cambridge geotechnical centrifuge operations. *Géotechnique* **30**, No. 3, 225–268.

Smith, A. K. C. & Bransby, P. I. (1976). The failure of reinforced earth walls by overturning. *Géotechnique* **26**, No. 2, 376–381.

Vidal, H. (1966). La terre armée. *Annls Inst. Tech. Bâtim.*, No. 223–224, Matériau 30.

Vidal, H. (1969). The principle of reinforced earth. *Highw. Res. Rec.*, No. 282.

Vidal, H. (1978). The development and future of Reinforced Earth. In *Proceedings of symposium on earth reinforcement*, pp 1–61. Pittsburgh: American Society of Civil Engineers.